

## Characterization of Protein Adsorption at the Phosphorylcholine Incorporated Polymer–Water Interface

E. F. Murphy and J. R. Lu\*

*Department of Chemistry, University of Surrey, Guildford GU2 5XH, UK*

A. L. Lewis, J. Brewer, J. Russell, and P. Stratford

*Biocompatibles Ltd., Farnham Business Park, Weydon Lane, Farnham, GU9 8QL, UK*

*Received September 28, 1999; Revised Manuscript Received February 14, 2000*

**ABSTRACT:** We have studied the adsorption of a number of model proteins onto the surface of a cross-linkable hydrogel polymer incorporated with phosphorylcholine (PC) groups and dodecyl chains (PC 100B). The structure of the coated thin polymer film was determined by neutron reflection combined with spectroscopic ellipsometry. No measurable change in the thickness of the polymer film was detected within the experimental time scale of minutes when immersed in water, showing a fast water solubilization process. The polymer film at the solid–water interface was modeled using a single layer of  $51 \pm 3$  Å with  $40 \pm 5\%$  water, suggesting a uniform distribution of water across the polymer film. This film structure is in sharp contrast with the uneven swelling of the film formed from a different hydrogel polymer (PC 100A) which had a similar molar ratio of dodecyl chains and PC groups but did not contain any silyl groups as cross-linkers. The results hence suggest that the uniform structure of the PC 100B film is rendered by the formation of the silyl cross-linking network. The effectiveness of the PC 100B film at reducing protein adsorption under different solution conditions was subsequently characterized. Both neutron reflection and spectroscopic ellipsometry showed substantial reduction in protein adsorption on PC 100B. At the bulk protein concentration around  $1 \text{ g dm}^{-3}$  the surface excess was found to be less than  $1 \text{ mg m}^{-2}$  for lysozyme and fibrinogen at pH 7 and BSA at pH 5, while under the same solution conditions, the surface excess at the hydrophilic silicon oxide–water interface was  $3.6 \pm 0.3 \text{ mg m}^{-2}$  for lysozyme,  $6.0 \pm 0.3 \text{ mg m}^{-2}$  for fibrinogen, and  $2.5 \pm 0.3 \text{ mg m}^{-2}$  for BSA. Despite the structural difference between the two coated polymer films, the residual level of protein adsorption was found to be comparable between the two PC polymer surfaces. The insensitivity of spectroscopic ellipsometry to the presence of a diffuse protein layer on the surface of the coated polymer films is also discussed.

### Introduction

Protein adsorption is a widespread interfacial phenomena occurring in the application of medical devices, in the processing of food and beverages, and in the bioseparation and bioengineering of proteins from blood. The extent of adsorption of protein molecules onto the surface of a given substrate is determined by a combined effect of the interaction between the protein molecules and the substrate surface and the interaction within the adsorbed protein layer.<sup>1–5</sup> The factors affecting these interactions include the properties of protein molecules such as size, shape, stability, charge and charge distribution; the solution properties such as protein concentration, pH, and ionic strength; and the physical nature of the solid substrate such as its hydrophobicity, charge, and charge density. The interplay between these factors has made it difficult to characterize the behavior of proteins at interfaces. Despite the complexity, electrostatic, hydrophobic, and entropic effects are often regarded as the main driving forces for surface adsorption. A hydrophobic surface can induce the deformation of globular protein and an eventual breakdown of the globular framework. Surface adsorption may lead to the direct contact of the hydrophobic moieties from protein molecules with the hydrophobic surface, resulting in the minimization of the exposure of the hydrophobic surface to water. The irreversible adsorption and the subsequent denaturation of globular proteins at the hydro-

phobic solid–water interfaces have been shown by many researchers using various methods.<sup>6–8</sup> At the hydrophilic solid–water interface, adsorption can be driven by charge-related electrostatic attraction and entropic effects arising from changes in conformational structure and hydration/dehydration of the solid substrate and protein molecules. Even in the absence of the effects of charge and conformational variation, adsorption can still be irreversible because the total number of contacts between protein molecules and the substrate is large and the change in solution conditions does not create enough driving force to overcome the energy barrier for desorption.

Adsorbed proteins may deteriorate and therefore cause further biological consequences. Many attempts have been made to reduce protein adsorption. Early studies have shown that the coating of polymers such as poly(vinyl chloride), poly(ethylene oxide), poly(etherurethane), poly(dimethylsiloxane), and poly(tetrafluoroethylene) onto solid substrates could reduce protein adsorption. However, since most of these polymers are not blood-compatible, their applications are limited. Recent research has led to the development of many new polymers that offer improved blood biocompatibility.<sup>9</sup> One of these new polymers is that studied in this work, and it has a polymethacrylate backbone bearing pendant alkyl chains, 2-hydroxypropyl groups, phosphorylcholine (PC) groups, and a small fraction of silyl groups as cross-linkers. Phosphorylcholine is the headgroup of phosphatidylcholine, the major component of the extracellular side of cell membranes. The fact that

\* To whom correspondence should be addressed.

proteins in the bloodstream do not foul onto the surface of cells shows that the outer surface of the cell walls, comprising PC groups, is biocompatible.<sup>10</sup> This work attempts to examine whether a similar effect is seen when the PC groups are incorporated into the synthetic polymer. Instead of using blood, we have performed the measurements using model proteins, including lysozyme, bovine serum albumin (BSA), and fibrinogen. These proteins represent a wide range of proteins found in body fluids with different physical properties. Furthermore, the basic information for these proteins such as their isoelectric points (IP), molecular weights, and their general solution behavior are well established.<sup>1,2</sup> Their adsorption behavior on different surfaces has also been studied by a number of techniques, and hence these results can be compared with those from our previous measurements. Our studies have shown that, in comparison with the level of adsorption of proteins onto several other model solid–water interfaces, the adsorption of these model proteins at the PC polymer–water interface has been substantially reduced.

## Experimental Section

Ellipsometric measurements were made on the Woollam variable angle spectroscopic ellipsometer 32 (WVASE32, manufactured by JA Woollam Co, Inc., USA) over a typical wavelength range of 300–700 nm. For a silicon substrate, the most sensitive variation in ellipsometric signal occurs at the incidence angle around 75°, and for this reason we will show the data collected at 75° only. The measurements have been made at both the air–solid and solid–liquid interfaces. In the case of measurements at the solid–water interface, a specially constructed sample cell was used. The polymer-coated silicon wafer is placed in the middle of the cell, and the measurement at the air–solid interface is usually made first before any aqueous solution is added for the solid–liquid experiment. The experimental geometry is such that the incoming beam enters the aqueous solution through a glass window and is reflected from the solid–water interface and exited from the opposite end through another glass window. The two windows on each side of the cell have been aligned at 75° with respect to the normal direction so that the incoming and exiting beams are always perpendicular to the window glasses. Thin glass slides were used as windows, and their effect on the incoming and exiting beams was calibrated at the beginning of the measurements.

Neutron reflection measurements were made on the white beam reflectometer CRISP at the Rutherford-Appleton Laboratory, ISIS, Didcot, UK,<sup>11</sup> using neutrons with wavelengths from 0.5 to 6.5 Å. A silicon block of dimensions 12.5 × 5 × 2.5 cm<sup>3</sup> was used, and the solution was held in a Teflon cell that was clamped against the large polished face of the silicon block. The neutron experiment used almost the same geometry as ellipsometry except the collimated beam was passed through the silicon block. Each reflectivity profile was measured at three different glancing angles, 0.35°, 0.8°, and 1.8°, and the results were combined. The absolute beam intensity was calibrated with respect to the intensity below the critical angle for total reflection at the silicon–D<sub>2</sub>O interface. A flat background, determined by extrapolation to high values of momentum transfer,  $\kappa$  ( $\kappa = (4\pi \sin \theta)/\lambda$ , where  $\lambda$  is the wavelength and  $\theta$  is the glancing angle of incidence), was subtracted. For all the measurements, the reflectivity profiles were essentially flat at  $\kappa > 0.15 \text{ Å}^{-1}$ , suggesting the attainment of a constant level of background.

The procedure for polishing and cleaning the large (111) face of the silicon block is the same as that described previously.<sup>12</sup> Silicon wafers (111) were also used in the ellipsometric measurements and were cleaned in the same manner as for the large neutron block. The uniformity of the oxide surfaces was usually checked by ellipsometry over spots at different locations, and for a given surface the oxide layer was always

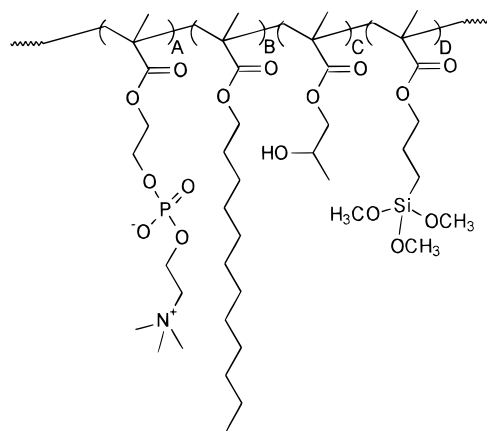


**Figure 1.** Molecular structure of PC 100B. The approximate mole fractions are 23% for A, 47% for B, 25% for C, and 5% for D. NMR analysis shows that the structure of fragment C containing a hydroxy group is predominantly in the form of 2-hydroxypropyl methacrylate with some 25% 1-methyl-2-hydroxyethyl methacrylate isomer.

$20 \pm 5 \text{ Å}$ . The error reflects the variation of the thicknesses obtained at different locations on the same surface. The surface hydrophilicity was checked by adsorption of  $1 \text{ g dm}^{-3}$  lysozyme at pH 7 in phosphate buffer with a total ionic strength of 0.02 M. The surface excess was always around  $3.6 \pm 0.3 \text{ mg m}^{-2}$ .

The thin polymer film was coated using a dip-coating device, and the detailed procedure has also been described previously.<sup>13</sup> Since the main composition of the polymer (PC 100B) used in this work is the same as PC 100A characterized in the previous study, almost identical coating conditions have been applied. The polymer was dissolved in the mixed solvent of ethanol and hexane (50 vol %), and the concentration was 0.1 wt %. The motor lifting speed was set at 5 mm/s, and this resulted in a film thickness of  $55 \pm 10 \text{ Å}$ . The coated surface was subsequently annealed at 70 °C under vacuum for 3.5 h. AFM (atomic force microscopy) showed that the annealing condition was sufficient to release the conformational stress within the film, rendering an improved uniformity on the outer surface.

PC 100B was copolymerized from mixed monomers of methacryloyloxyethylphosphorylcholine (MPC), lauryl methacrylate (LM), 2-hydroxypropyl methacrylate (HPM), and trimethoxysilylpropyl methacrylate (TPM). The chemical structure of PC 100B is in the form of a methacrylate backbone grafted with LM, MPC, HPM, and TPM. The schematic configuration of PC 100B is shown in Figure 1. The main difference between this polymer and PC 100A studied in our previous work is the introduction of some 25% hydroxypropyl groups and 5% silyl groups. The latter works as cross-linkers within the polymer once the film is formed. Although the inclusion of the two new functional groups means that the total contents of MPC and LM have to be reduced, the molar ratio of MPC to LM is still kept constant at 1:2. The annealing at 70 °C under vacuum improves the formation of the silyl network. The procedure for synthesis and purification has been described in refs 14. PC 100B is a typical cross-linkable copolymer from the MPC-LM series and is in some cases also referred to as PC1036.

Chicken egg white lysozyme (Sigma, 99%+, catalog no. L6876) was used as supplied. Lysozyme has an isoelectric point around pH 11. Its globular structure is roughly ellipsoidal and has an approximate dimension of  $30 \times 30 \times 45 \text{ Å}^3$ . BSA (Sigma, catalog no. A0281) was fatty acid-free and was also used as supplied. Its isoelectric point was about pH 4.8, and the globular dimension is about  $40 \times 40 \times 140 \text{ Å}^3$ . Fibrinogen (Sigma, catalog no. F8630, from bovine plasma) is known as a blood clotting agent and has an isoelectric point of 5.5. Adsorption measurements were made at pH 7 for lysozyme and fibrinogen and at pH 5 for BSA, all at 298 K. The solution pH was adjusted using phosphate buffer ( $\text{Na}_2\text{HPO}_4$  and  $\text{NaH}_2\text{PO}_4$ ), and the total ionic strength at each pH was fixed at 0.02

M for lysozyme and BSA solutions. For fibrinogen solutions, the total ionic strength for phosphate buffer was controlled at 0.05 M. To aid the dissolution of fibrinogen, additional sodium chloride was added to a concentration level of 0.1 M. There were small differences in the pH between H<sub>2</sub>O and D<sub>2</sub>O solutions, but these were adjusted to be the same within an accuracy of 0.2 pH units. High-purity Elgastat water (UHQ) was used throughout the work, and D<sub>2</sub>O was purchased from Sigma and was used as supplied. The surface tension of H<sub>2</sub>O and D<sub>2</sub>O was typically over 71 mN m<sup>-1</sup> at 298 K, indicating the absence of any surface active impurity. The glassware and Teflon troughs for the reflection measurements were cleaned using alkaline detergent (Decon 90) followed by repeated washing in UHQ water.

## Results

**(A) Ellipsometric Measurements.** In a spectroscopic measurement, the two ellipsometric angles,  $\Psi$  and  $\Delta$ , are usually recorded as a function of wavelength,  $\lambda$ .  $\Psi$  measures the change in the amplitude of the polarized beam after reflection while  $\Delta$  measures the change in phase. Structural information with respect to the direction normal to the surface is usually obtained by fitting refractive index profiles to  $\Psi$  and  $\Delta$  simultaneously using the optical matrix formula. The variation of refractive index with  $\lambda$  is taken into account using the Cauchy equation.<sup>15</sup>

Because the native oxide layer present on the surface of the silicon block contributes to the signal in ellipsometric measurements, its thickness,  $\tau$ , was usually measured before the polymeric thin layer was coated. The measurements were made at the air–solid interface over the wavelength range of 300–700 nm at the incidence angle of 75°. The simultaneous fitting to the profiles of  $\Psi$  and  $\Delta$  using a uniform layer model gave a value of  $\tau$  of  $23 \pm 3$  Å, with the refractive index,  $n$ , for the oxide layer taken to be the same as its bulk value. We have shown in the previous work that the assumption of no defects within the oxide layer is reasonable.<sup>3,4,12</sup> No roughness was used in the fitting. Repeated measurements were performed on several other spots on the same oxide surface, and the thicknesses of the oxide layer were found to be the same within the quoted error, suggesting that the bare oxide surface is smooth.

The thickness of the coated polymer layer at the air–solid interface was subsequently determined using the same measurement procedure. The simultaneous fitting to  $\Psi$  and  $\Delta$  was made by taking the structure of the underlying oxide to be unaffected by the coating and the refractive index of the polymer layer to be the same as its bulk value. This led to the value of  $55 \pm 5$  Å for the polymer film. If both  $\tau$  and  $n$  were varied in the fitting, the range of the variation in  $\tau$  was around  $\pm 10$  Å. Although thicknesses beyond this range might also fit the measured data, the corresponding refractive indices were physically unreasonable. This situation was mainly caused by the coupling between  $\tau$  and  $n$  when the layer is ultrathin, typically under 300 Å, as has been discussed previously.<sup>12</sup> The uniformity of the coated film was characterized by repeating the same measurements over six different spots on the same surface over an area of  $2 \times 8$  cm<sup>2</sup> in the central area of the coated surface. It was found that the thickness of the polymer layer was constant at  $55 \pm 5$  Å when the refractive index was fixed at the bulk value for the polymer, suggesting that the film was reasonably uniform.

As the polymer contains a large fraction of hydroxyl and PC groups, it is likely to swell when immersed in

the buffered water. The possible swelling of the ultrathin polymer film with time was followed by monitoring the variation of  $\Psi$  and  $\Delta$  with time at the solid–water interface. As described previously, the beam was directed into the aqueous solution through a glass window, was reflected from the solid–water interface, and exited from the opposite side of the window. The measurements were again made over the wavelength range of 300–700 nm, and each single scan was done in less than 2 min. The measurements were repeated over a period of 15 h, and no time dependent variation was observed, showing that if any swelling occurred it must be within the first spectroscopic scan of about 2 min. A similar coupling effect was observed between the layer thickness and refractive index at the solid–water interface. As in the case of fitting at the air–solid interface, if both  $\tau$  and  $n$  were varied, a wide range of  $\tau$  could be used to fit the measured profiles at the solid–water interface. If no swelling was assumed and the refractive index for the layer was taken to be the same as that for the bulk polymer, the thickness for the polymer layer was calculated to be around 50 Å, as expected. If it was assumed that there was 50% water in the layer and the effect of water mixing on the refractive index was taken into account by the effective medium approximation (EMA),<sup>15</sup> a thickness of  $50 \pm 5$  Å would still produce a good fit to the measured data, showing that under these conditions the ellipsometric measurements are insensitive to the possible swelling of the ultrathin film. It should be pointed out, however, that although it is difficult to decouple the two structural parameters, the measurements are very sensitive to the product of the two, as is evident from the large variations in  $\Psi$  and  $\Delta$  with and without the coated thin film (Figure 2).

The adsorption experiment was subsequently carried out by replacing the buffered water with protein solution. For lysozyme, the measurement was made at pH 7 and at the lysozyme concentrations of 0.03, 1, and 4 g dm<sup>-3</sup>. Figure 2 shows the measured ellipsometric profiles of  $\Psi$  and  $\Delta$  in the presence of 4 g dm<sup>-3</sup> lysozyme, as compared with the profiles obtained at the polymer–water interface. It can be seen from Figure 2 that the two sets of profiles are virtually identical within the experimental error, suggesting little adsorption of lysozyme. Similar measurements were also made for the adsorption of BSA and fibrinogen. No measurable amount of protein was detected in either case. The adsorption of BSA was carried out at pH 5 at the BSA concentrations of 0.05 and 2 g dm<sup>-3</sup>, and for fibrinogen the measurements were made at pH 7 and at the fibrinogen concentrations of 0.1 and 1 g dm<sup>-3</sup>. The reliability and implication of these ellipsometric measurements will be further discussed after the results from neutron reflection are presented.

**(B) Neutron Reflection Measurements.** Neutron reflection has two major advantages over spectroscopic ellipsometry. The first is the much shorter wavelength of neutron beam sources, which makes neutron measurements more sensitive to the smaller dimension of the interfacial layers. The second is the use of isotopic substitution, which is achieved by varying the ratio of H<sub>2</sub>O and D<sub>2</sub>O in this work. The concept of isotopic substitution is based on the fact that neutron reflectivity, defined as the ratio of the reflected beam intensity to that of the incoming one, is affected by scattering lengths which vary from element to element. Because



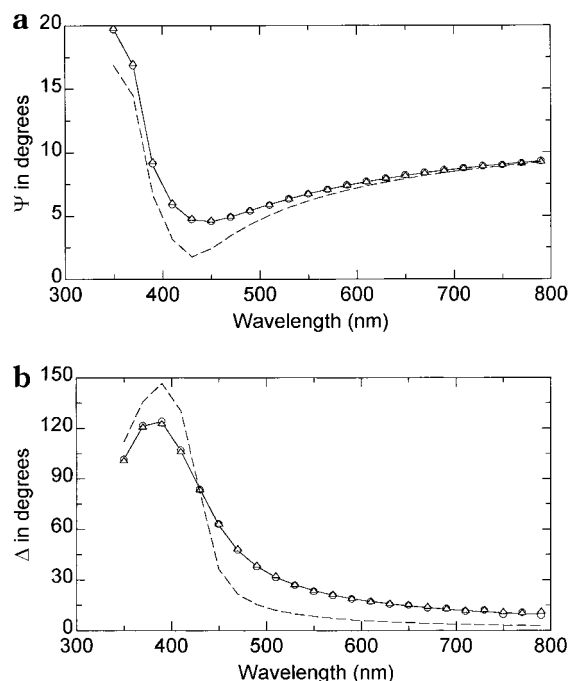


**Figure 2.** Plots of  $\Psi$  (a) and  $\Delta$  (b) as a function of  $\lambda$  at the PC 100B-coated solid–water interface in the presence ( $\Delta$ ) and absence ( $\circ$ ) of  $4 \text{ g dm}^{-3}$  lysozyme at pH 7. The measurements were made at the incidence angle of  $75^\circ$  and at  $25^\circ \text{C}$ . The continuous lines were calculated using the optical matrix formula assuming an oxide layer thickness of  $23 \pm 3 \text{ \AA}$  and a polymeric film of  $51 \pm 3 \text{ \AA}$ . That the two measured profiles are identical, suggesting little protein adsorption. The dashed lines were the measured  $\Psi$  and  $\Delta$  at the underlying silicon oxide–water interface.

the scattering lengths for hydrogen and deuterium are of opposite sign, the scattering lengths for  $\text{H}_2\text{O}$  and  $\text{D}_2\text{O}$  are also of opposite sign. The variation in the ratio of  $\text{H}_2\text{O}$  to  $\text{D}_2\text{O}$  alters neutron reflectivity and hence serves to highlight the interfacial structure differently. The combined measurements under different water contrasts lead to the improved interfacial resolution.

Neutron reflection measurements were first made to determine the thickness and composition of the oxide layer. As previously explained,<sup>16,17</sup> neutron reflectivity is directly related to the scattering length density profile along the surface normal direction. The relationship between the scattering length density,  $\rho$ , and the scattering lengths of the components within the layer can be expressed as

$$\rho = \sum m_i b_i \quad (1)$$

where  $m_i$  is the number density of element  $i$  and  $b_i$  is its scattering amplitude (scattering length). For the characterization of the bare oxide layer, neutron reflectivity profiles were measured under  $\text{D}_2\text{O}$  and CMSi ( $\text{D}_2\text{O}:\text{H}_2\text{O} \approx 1:2$ ). The results were analyzed using the optical matrix formula, and the fitting produced a value of  $\tau$  of  $20 \pm 3 \text{ \AA}$  and  $\rho = 3.4 \times 10^{-6} \text{ \AA}^{-2}$  for the oxide layer, suggesting a negligible amount of water in the oxide layer. These results offer support for the assumption of no defects within the oxide layer made in the treatment of ellipsometry data, and the thicknesses obtained from the two techniques are consistent with each other.

The structure of the coated polymer film was measured under  $\text{D}_2\text{O}$  and CM4 ( $\text{D}_2\text{O}:\text{H}_2\text{O} = 3:1$  and  $\rho \approx 4$

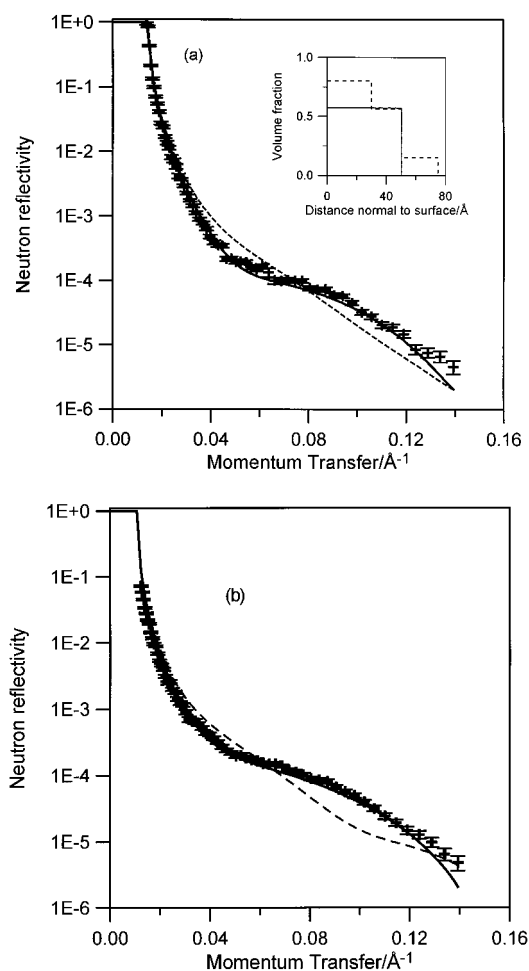


**Figure 3.** Neutron reflectivity profiles measured from the PC 100B-coated solid–water interface. The continuous lines were calculated using the thickness of  $51 \pm 3 \text{ \AA}$  for the polymer film with 41% water, and the dashed lines were calculated using the volume fraction distribution obtained for PC 100A. The solvent is  $\text{D}_2\text{O}$  in (a) and is CM4 ( $\text{D}_2\text{O}:\text{H}_2\text{O} = 3:1$ ) in (b). The volume fraction distributions for the two polymers are inserted in (a) for comparison. The thicknesses of the silicon oxide layers were taken to be  $20 \pm 3 \text{ \AA}$ .

$\times 10^{-6} \text{ \AA}^{-2}$ ), and the resultant reflectivity profiles are shown in Figure 3. Before any elaborate models are used to fit the reflectivity profiles, it is useful to test whether the uniform layer model corresponding to that obtained from the ellipsometric profiles would fit the neutron data. The continuous lines shown in Figure 3 were calculated assuming a thickness of  $51 \pm 3 \text{ \AA}$  for the polymer layer. The corresponding values of  $\rho$  for the bulk phase had to be varied to reflect the change in the contrast of the bulk solvent. The deviation of the value of  $\rho$  for the interfacial film from that of pure polymer reflects the extent of solubilization of water into the polymer film, and the exact relationship can be expressed as

$$\rho = \rho_p x_p + \rho_w (1 - x_p) \quad (2)$$

where  $\rho_p$  and  $\rho_w$  are the scattering length densities for the polymer and water and  $x_p$  is the volume fraction of the polymer in the layer. For PC 100B,  $\rho_p = 4.8 \times 10^{-7} \text{ \AA}^{-2}$ . The value of  $\rho$  was found to be  $2.9 \times 10^{-6} \text{ \AA}^{-2}$  from the fitting to the reflectivity in  $\text{D}_2\text{O}$ , and from eq 2  $x_p$  was calculated to be 0.58. Likewise,  $x_p$  could also be calculated from the fitted  $\rho$  to the reflectivity profile in

CM4, and the value was found to be 0.62. As the difference is within the acceptable error, we can conclude that the final volume fraction of water within the layer is  $0.4 \pm 0.05$ .

Despite the formation of the silyl cross-linking network, the mixing of some 40% water into the polymer film is expected to cause the expansion of the film along the surface normal direction and hence an increased layer thickness. Since the ellipsometric measurement at the air–solid interface offers a thickness of  $55 \pm 5$  Å for the dry film, which is close to that obtained from neutron reflection at the solid–water interface, the combined results tend to indicate that such a large extent of water solubilization did not cause any measurable amount of increment in the polymer film thickness. As already indicated above, the thickness obtained from the ellipsometric measurement suffers from the coupling problem, and caution should be taken in comparing the two sets of data. Hence, the reliability of the ellipsometric thicknesses is heavily affected by the values of refractive indices assumed for the polymer films. Ideally, parallel neutron reflection measurements should be made at the air–solid interface to obtain the dry film thickness, but for the fully hydrogenated polymer, the measurement is insensitive to the polymer film thickness at the air–solid interface because the scattering length density of the polymer layer is close to zero. However, at the solid–D<sub>2</sub>O interface the hydrogenated polymer layer is highlighted by the contrast of the bulk solvent. The calculated reflectivity profiles shown in Figure 3a,b fit the measured ones well under both water contrasts, showing that the uniform layer model is appropriate for describing the distributions of the polymer and water across the film. The sensitivity of the fits to the polymer film thickness can be demonstrated by varying the thickness in the model fitting while fixing the water volume fraction at 0.4. Obvious deviations occur between the calculated and measured reflectivity profiles when the thickness is beyond the range of 47–54 Å, suggesting that neutron measurement offers greater sensitivity to the dimension of the layer.

In a previous study<sup>12</sup> we have characterized the structure of the polymer film formed by PC 100A. As already indicated, the main difference in chemical structure between the two polymers is the absence of 5% silyl groups in PC 100A. Other differences, e.g., the presence of hydroxyl groups, is not expected to affect the main structure of the polymer film. The possible swelling with time was also monitored using ellipsometry. Again, no observable change was detected for the ultrathin films under 100 Å within the time scale of 1 min. However, the equilibrated volume fraction distributions for the two polymer films were found to differ dramatically. While PC 100B swelled uniformly, very uneven swelling occurred in PC 100A. The dashed lines in Figure 3a,b were calculated from the best fit to the measured reflectivities for PC 100A under the two water contrasts after the film was saturated with water. The model contains three layers; the inner layer closest to the solid substrate is about  $30 \pm 3$  Å thick and contains some 80% polymer; the middle layer is about  $20 \pm 3$  Å thick and contains some 55% polymer; the outer layer is about  $25 \pm 5$  Å thick and contains some 15% polymer. In contrast, the swollen PC 100B layer is about 50 Å thick, and the density distributions for both polymer and water are uniform throughout the film. The volume

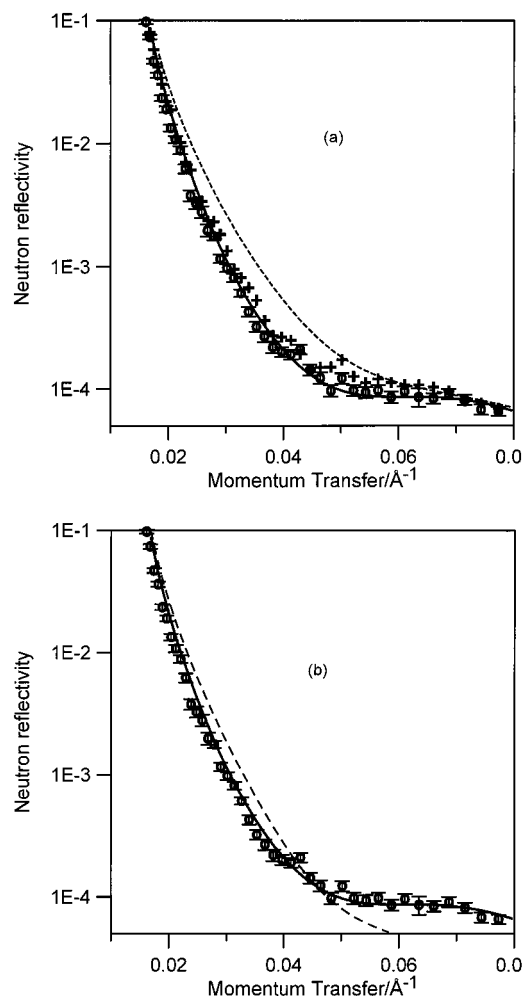


**Figure 4.** Neutron reflectivity profiles measured from the PC 100B-coated solid–D<sub>2</sub>O interface at the lysozyme concentrations of 1 g dm<sup>−3</sup> (+) and 4 g dm<sup>−3</sup> (○). The continuous lines are the best fit to the measured profile at 4 g dm<sup>−3</sup>, giving a surface excess of  $1.7 \pm 0.3$  mg m<sup>−2</sup> and layer thickness of  $90 \pm 10$  Å. The dashed line in (a) was measured from the polymer-coated solid–buffered D<sub>2</sub>O interface and was shown to indicate the level of lysozyme adsorption. The dashed line in (b) was calculated assuming the lysozyme layer was only 45 Å, and the deviation clearly indicates that the lysozyme layer has to be thicker.

fraction distributions for the two polymers are inserted in Figure 3a. The uniform density distribution in PC 100B must be caused by the formation of the silyl network.

The adsorption of lysozyme onto the PC 100B surface at varying lysozyme concentrations was measured in the buffered D<sub>2</sub>O at pH 7, and the reflectivity profiles are shown in Figure 4a. The reflectivity profile from the solid polymer-buffered D<sub>2</sub>O interface is also shown, and the difference indicates the extent of lysozyme adsorption. At 0.03 g dm<sup>−3</sup> (not shown for clarity) the reflectivity profile changes a little from that of buffered D<sub>2</sub>O, suggesting that there is a very small amount of lysozyme adsorption. However, at 1 g dm<sup>−3</sup>, a relatively large deviation occurs, indicating more lysozyme adsorption. As the lysozyme concentration is further increased to 4 g dm<sup>−3</sup>, the reflectivity is shifted slightly further from the buffered D<sub>2</sub>O profile, indicating a further increase in lysozyme adsorption with the bulk concentration.

Quantitative information about the surface excess of lysozyme was obtained by fitting models to the adsorbed

layers. It was assumed that protein adsorption does not alter the structure of the oxide and polymer layers, and the difference between the measured profiles in the presence of lysozyme and that of the buffered D<sub>2</sub>O has to be accounted for by the adsorbed lysozyme layer. In the case of lysozyme adsorption onto the hydrophilic silicon oxide–water interface, we found that lysozyme molecules prefer to adopt well-structured conformations, and the thicknesses of the layers are comparable to the dimension of the globular structure for lysozyme.<sup>4,18</sup> Because the outer surface of PC 100B is uniform, it is interesting to examine whether the thickness of the adsorbed layer is close to any of the axial lengths for lysozyme. Since the amount of lysozyme adsorbed is less than a close packed monolayer, we have tried to fit the reflectivity profiles by constraining the lysozyme layer thickness to within 45 Å (the long axial length) and allowing  $\rho$  to vary to obtain the best fit. Figure 4b shows the fit to the measured profile at 4 g dm<sup>-3</sup> with the lysozyme layer thickness fixed at 45 Å (dashed line). Because the broad interference fringe occurs at the higher  $\kappa$  than that of the measured profile, it is clear that a thickness of 45 Å is too short to account for the distribution of the adsorbed lysozyme. Once it is decided to give up the constraint to the thickness of lysozyme layer, it is relatively straightforward to analyze the measured neutron data. The reflectivity profiles are best fitted by a uniform layer distribution with the thickness of  $90 \pm 10$  Å. The lysozyme volume fraction within the layer is  $0.09 \pm 0.03$  at 1 g dm<sup>-3</sup> and  $0.13 \pm 0.03$  at 4 g dm<sup>-3</sup>. Under the condition of uniform layer distribution, the surface excess,  $\Gamma$ , can be deduced directly from the derived scattering length density ( $\rho$ ) and thickness of the layer ( $\tau$ ) using

$$\Gamma = \frac{\tau(1 - x_p)}{n_w V_w N_a} \quad (3)$$

where  $\tau$  is the thickness of the protein layer,  $n_w$  is the number of water molecules associated with each protein molecule,  $V_w$  is the molecular volume of water, and  $N_a$  is Avogadro's constant. The value of  $n_w$  can be evaluated from the following equation

$$n_w = \frac{(1 - x_p)b_p}{\rho V_w - b_w(1 - x_p)} \quad (4)$$

where  $b_w$  and  $b_p$  are the scattering lengths for water and protein. For lysozyme, the total scattering length  $b_p$  in D<sub>2</sub>O is 0.061 Å and that in CM4 is 0.052 Å, assuming complete exchange between labile hydrogens within lysozyme and water. We have previously discussed that any incomplete exchange is not going to cause any measurable error to the surface excess, partly because labile hydrogens only contribute to a fraction of the total scattering length and partly because sufficient experimental evidence has shown that over 80% labile hydrogens will exchange within the time scale of the experiment. From eq 3 the surface excess is calculated to be  $1.2 \pm 0.3$  mg m<sup>-2</sup> at 1 g dm<sup>-3</sup> and  $1.7 \pm 0.3$  mg m<sup>-2</sup> at 4 g dm<sup>-3</sup>. For clarity, only the best fit to the measured reflectivity profile at 4 g dm<sup>-3</sup> is shown in Figure 4a. The scales in Figure 4 have also been expanded to show the region where the main difference occurs between reflectivities.

We recall the ellipsometric measurements shown in Figure 2 that show no difference between the ellipso-

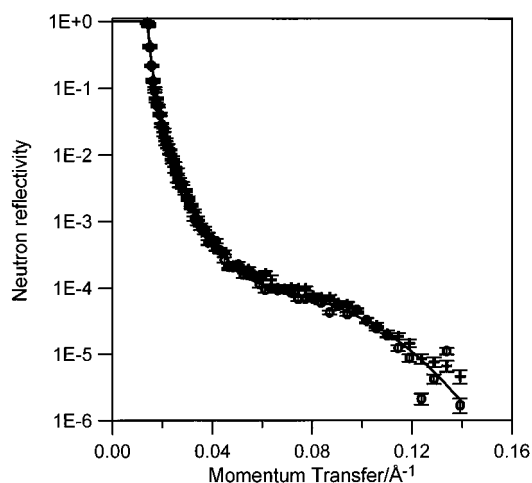


**Figure 5.** Neutron reflectivity profiles measured from the PC 100B-coated solid–D<sub>2</sub>O interface before (○) and after (+) lysozyme adsorption. The continuous line was the best fit assuming the polymer layer is  $51 \pm 3$  Å thick and contains 41% water. The results suggest that the adsorbed lysozyme was completely removed after in contact with the cationic surfactant C<sub>12</sub>TAB and that the polymer film remained intact during the course of the experiment despite the high percentage of water in it.

metric profiles in the presence and absence of lysozyme, hence indicating little adsorption. These results appear to contradict the findings from neutron reflection. This issue will be addressed later, but it is worthwhile to indicate at this stage that the apparent discrepancy is caused by the insensitivity of ellipsometry to the diffuse distribution of the protein layer.

It is of interest to examine whether the adsorbed protein can be removed and the polymer surface can be regenerated. We have first tried to remove the adsorbed lysozyme by rinsing the polymer surface with buffered D<sub>2</sub>O. The subsequent neutron measurement at the solid–D<sub>2</sub>O interface showed an almost identical reflectivity profile to that before rinsing, showing that the majority of the adsorbed lysozyme still remained after rinsing. This suggests that the adsorption is irreversible with respect to protein concentration, a trend similar to that observed on PC 100A and the surface of the hydrophilic silicon oxide.<sup>3,4,12</sup> Further removal of the adsorbed residue was carried out by rinsing the surface with the solution of dodecyl trimethylammonium bromide (C<sub>12</sub>TAB) with its concentration just above its critical micellar concentration ( $\text{cmc} = 14 \times 10^{-3}$  M). The surface was then rinsed with buffered D<sub>2</sub>O before a repeated reflection measurement was made at the solid–D<sub>2</sub>O interface. Shown in Figure 5 is the reflectivity obtained at the solid polymer–D<sub>2</sub>O interface after the surface was cleaned with the surfactant, as compared with the one measured before lysozyme adsorption. The two reflectivity profiles are virtually overlapping, showing that the adsorbed lysozyme was completely removed from the coated polymer by C<sub>12</sub>TAB. These results also suggest that despite a large volume fraction of water solubilized into the polymer film, its structure remained intact during the course of the experiment. This finding is important for the applications of the polymer in medical and industrial coatings.

A further adsorption experiment was made using BSA. Despite being globular, BSA is much greater in size and is less stable than lysozyme. The flexibility of BSA mainly arises from the connection of the three main domains through physical forces. The six subdomains



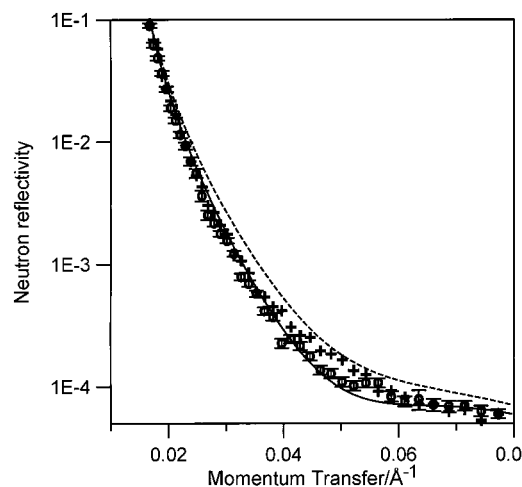


**Figure 6.** Neutron reflectivity measured from the PC 100B-coated solid–D<sub>2</sub>O interface after adsorption of BSA onto the polymer surface at 0.05 g dm<sup>-3</sup> (+) and 2 g dm<sup>-3</sup> (O). The profile at 0.05 g dm<sup>-3</sup> is close to that from the polymer-coated solid–buffered D<sub>2</sub>O interface (dashed line), suggesting that the adsorbed amount is small. The continuous line is the fit to the measured profile at 2 g dm<sup>-3</sup>, giving a surface excess of  $1.0 \pm 0.3$  mg m<sup>-2</sup>.

are however more tightly bound through the 17 disulfide bridges. The adsorption isotherm of BSA on many model substrates including polystyrene and poly(methyl methacrylate) (PMMA) is characterized by the attainment of the maximum surface excess around 2–3 mg m<sup>-2</sup> at very low bulk concentration, suggesting a very high surface activity.<sup>1,19</sup> It is hence interesting to examine how BSA behaves on the PC polymer surface.

Adsorption of BSA onto PC 100B was studied by neutron reflection at pH 5 and at the bulk concentrations of 0.05 and 2 g dm<sup>-3</sup>. Figure 6 shows the measured reflectivity profiles together with the best fit to the measured one at 2 g dm<sup>-3</sup>. The reflectivity obtained from the solid polymer–buffered D<sub>2</sub>O interface is also shown to indicate the shift of the reflectivity profiles caused by BSA adsorption. The surface excess at 0.05 g dm<sup>-3</sup> was found to be  $0.5 \pm 0.3$  mg m<sup>-2</sup> from the model fitting and that at 2 g dm<sup>-3</sup> to be  $1.0 \pm 0.3$  mg m<sup>-2</sup>, with a total layer thickness around  $60 \pm 10$  Å. It was found that the measured profile at 2 g dm<sup>-3</sup> was better fitted with a two-layer model. The fitting shown in Figure 6 was obtained by dividing the total distribution into two layers of 30 Å each. The protein volume fraction for the inner layer was found to be  $0.1 \pm 0.03$  and that for the outer layer to be  $0.05 \pm 0.03$ . The adsorbed BSA layer was also rinsed by the C<sub>12</sub>TAB solution, and complete removal of the protein was obtained.

We have also tested the effectiveness of the PC polymer-coated surface in reducing fibrinogen adsorption. Fibrinogen is a blood-clotting protein and is also very surface active.<sup>2,20</sup> Its adsorption on the surface of PC 100B has been characterized at the fibrinogen concentration of 0.1 and 1 g dm<sup>-3</sup>, and the solution pH was controlled at 7. The reflectivity profile in the presence and absence of 1 g dm<sup>-3</sup> fibrinogen is shown in Figure 7, and the narrow gap between the two reflectivity profiles shows that the extent of adsorption is very small. At 0.1 g dm<sup>-3</sup>, the reflectivity profile is virtually identical to that from the pure buffer, showing negligible adsorption. At the higher fibrinogen concentration, the surface excess was estimated to be  $0.8 \pm 0.3$  mg m<sup>-2</sup>. The adsorbed protein layer is again very

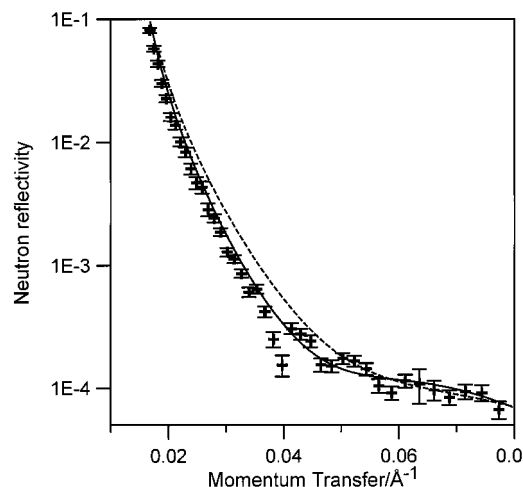


**Figure 7.** Neutron reflectivity measured from the PC 100B-coated solid–D<sub>2</sub>O interface after adsorption of fibrinogen onto the polymer surface at 1 g dm<sup>-3</sup> (+), as compared with the reflectivity measured from the polymer-coated solid–buffered D<sub>2</sub>O interface (dashed line). The fitting (continuous line) gives a surface excess of  $1.0 \pm 0.3$  mg m<sup>-2</sup>.

broad, and the best fitted layer is  $100 \pm 10$  Å thick. The volume fraction of the protein within the layer is hence less than 5%. As in the cases of lysozyme and BSA, the adsorbed fibrinogen can also be removed by rinsing the polymer surface with C<sub>12</sub>TAB solution, but complete removal was only achieved after several times of repeated rinsing with the surfactant solution.

## Discussion

We first discuss the apparent discrepancy in the amount of protein adsorbed at the PC 100B–water interface between the two techniques. The results from neutron reflection have indicated that all the adsorbed proteins are distributed over a wide depth range along the surface normal direction, and yet the volume fractions of the proteins within the adsorbed layers remain very low. In most cases the volume fractions are under 10%. Such diffuse protein layer distributions are relatively easy for neutron reflection to detect because of the high contrast created by the use of D<sub>2</sub>O as a solvent. However, the alteration of the refractive index profile across the interface arising from the presence of 10% diffuse protein layer is relatively small, and its effect on  $\Psi$  and  $\Delta$  is hence not appreciable. Since we have already shown the almost identical ellipsometry profiles with and without lysozyme in Figure 2, we compare in Figure 8 the calculated  $\Psi$  and  $\Delta$  by taking into consideration the 10% lysozyme layer of 90 Å thick (continuous lines) with the actual measured ones under 4 g dm<sup>-3</sup> lysozyme. The two sets of the curves are again identical, suggesting that under these conditions ellipsometry is unable to detect the presence of such a diffuse protein layer. For the adsorption at the PC 100A–solution interface studied in our previous work, the discrepancy between the two methods was less. This is because the outer surface of PC 100A was very rough, and the adsorbed protein layer was heavily mixed with the polymer. Under this condition, the ellipsometric measurement appeared to give a better estimate of the surface excesses although the values from ellipsometric measurement were still lower than those from neutron reflection (see Tables 1–3).

We have recently studied the adsorption of the three model proteins on a number of model substrate sur-

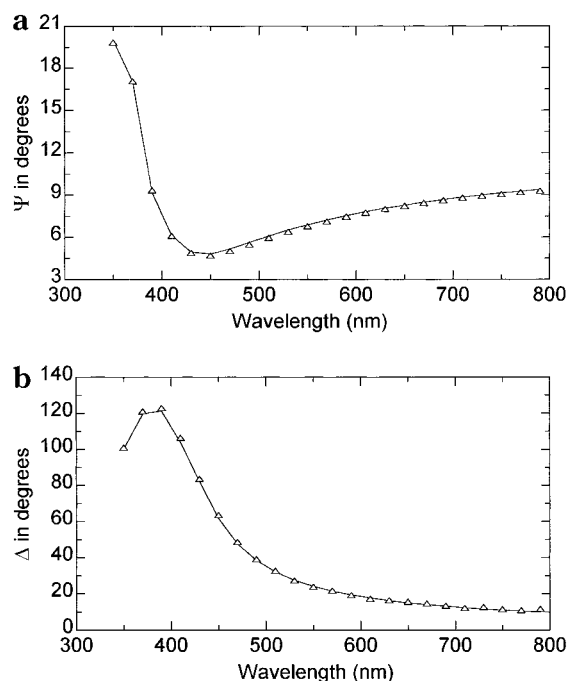


**Figure 8.** Comparison of the measured  $\Psi$  (a) and  $\Delta$  (b) for  $4 \text{ g dm}^{-3}$  lysozyme with those calculated by taking into account the  $90 \text{ \AA}$  diffuse layer as determined from neutron reflection (continuous lines). Little difference exists between the two sets of ellipsometric profiles, showing that the ellipsometric measurement is insensitive to the presence of such a diffuse protein layer.

**Table 1. Comparison of Lysozyme Surface Excesses Adsorbed at Different Solid–Water Interfaces at pH 7**

substrate	$C/\text{g dm}^{-3}$	$\Gamma \pm 0.4/\text{mg m}^{-2}$ (ellipsometry)	$\Gamma \pm 0.2/\text{mg m}^{-2}$ (neutron)
PC 100B	0.03	0	0.3
	1	0	1.2
	4	0	1.7
PC 100A	0.03	0	0.3
	1	0.3	0.7
	4	1.3	1.9
$\text{SiO}_2$	0.03	1.1	1.0
	1	3.5	3.7
	4	4.6	4.8
PMMA	0.03	0.5	
	1	2.0	
	4	2.6	
OTS	0.03	1.9	1.7

**Table 2. Comparison of BSA Surface Excesses Adsorbed at Different Solid–Water Interfaces at pH 5**

substrate	$C/\text{g dm}^{-3}$	$\Gamma \pm 0.4/\text{mg m}^{-2}$ (ellipsometry)	$\Gamma \pm 0.3/\text{mg m}^{-2}$ (neutron)
PC 100B	0.05	0	0.4
	2	0	1.0
PC 100A	0.05	0.3	0.5
	2	1.0	1.2
$\text{SiO}_2$	0.05	1.5	2.0
	2	3.0	2.8
PMMA	0.05	1.3	
	2	2.3	
OTS	0.05	2.0	

faces,<sup>21</sup> and the results are summarized in Tables 1–3, together with the surface excesses on the two PC polymer surfaces. For lysozyme adsorption on silicon oxide and OTS, measurements have been made using both neutron reflection and spectroscopic ellipsometry. There is a good agreement between the parallel measurements using the two methods, suggesting that although ellipsometry is insensitive to the very diffuse

**Table 3. Comparison of Fibrinogen Surface Excesses Adsorbed at Different Solid–Water Interfaces at pH 7**

substrate	$C/\text{g dm}^{-3}$	$\Gamma \pm 0.4/\text{mg m}^{-2}$ (ellipsometry)	$\Gamma \pm 0.2/\text{mg m}^{-2}$ (neutron)
PC 100B	0.1	0	0.3
	1	0	0.8
PC 100A	0.1	0.7	0.5
	1	0.7	0.7
$\text{SiO}_2$	0.1	5.6	
	1	6.0	
PMMA	0.1	2.5	
	1	2.0	
OTS	0.1	5.0	

protein layers on the surface of PC 100B, it offers a reasonable estimate of the adsorption that is dominated by the dense protein layers. The hydrophobed silicon oxide surface was formed by coating a self-assembled monolayer of octadecyltrichlorosilane (OTS) onto the freshly cleaned silicon oxide surface.<sup>22</sup> The PMMA surface was obtained by coating a thin and smooth layer of PMMA of some  $50 \text{ \AA}$  thick on the surface of silicon oxide. Although no neutron measurement was made for the adsorption of all three proteins at the PMMA–solution interface, the good consistency observed on the surfaces of silicon oxide and OTS shows that the ellipsometric surface excesses are sufficiently accurate for the purpose of comparison.

The results shown in Tables 1–3 show that the nature of the surfaces has a drastic effect on the level of protein adsorption. The two PC polymer-coated surfaces show the least amount of adsorption at a given protein concentration. This is so for all the three proteins studied. While the surface excess shows a clear trend of increase with the size and flexibility of the protein molecules on all other model surfaces studied, an opposite trend is observed for the adsorption on the two PC polymers, suggesting that the PC polymer surfaces are most effective at deterring the adsorption of large fibrous proteins.

Several studies have been made in the literature to characterize the adsorption of these proteins onto different interfaces. A number of ellipsometry measurements have produced the surface excess between  $2.5$  and  $3.5 \text{ mg m}^{-2}$  for the adsorption of  $1 \text{ g dm}^{-3}$  lysozyme at the silicon oxide–water interface with the total ionic strength below  $0.05 \text{ M}$ ,<sup>23–25</sup> broadly consistent with the value of  $3.5 \text{ mg m}^{-2}$  obtained from our measurements. Some experiments have also been made to quantify the level of lysozyme adsorbed onto various polymer–water interfaces. For example, lysozyme adsorption onto neutral and charged polystyrene particles has been studied by Haynes et al.<sup>26</sup> and Fair et al.<sup>27</sup> The surface excess was found to be between  $2$  and  $3 \text{ mg m}^{-2}$  at a lysozyme concentration around  $1 \text{ g dm}^{-3}$ . Similar studies have been made on the adsorption of BSA onto a number of polymeric and metal oxide substrates,<sup>2</sup> and the surface excess was typically found to attain a value between  $2$  and  $3 \text{ mg m}^{-2}$  at a very low BSA concentration, equivalent to the formation of a full monolayer coverage. All these results reinforce the fact that the surface excesses on bare oxide and other polymer surfaces are much higher than those adsorbed on the two PC polymers.

Although the structures of the two PC polymer films are very different, the surface excesses are comparable under a given bulk solution condition. This observation may suggest that despite the difference in the chemical constituents between the two polymers, the composition



of the outer surfaces for the two polymer films must be close. The formation of the silyl network is clearly important for the stabilization of the coated film, but it has no obvious effect on protein adsorption. Since both polymers contain PC and dodecyl chain groups, the reduced adsorption tends to suggest that the polymer surfaces are composed of either PC groups or a mixture of PC and dodecyl chains. The hydroxyl groups in PC 100B either do not have any profound effect on protein adsorption or are not present at the interface. The advancing contact angles for the two polymer surfaces were found to be rather high, and the values were around  $75 \pm 5^\circ$ . This observation tends to suggest that the surfaces are composed of a mixture of PC groups and dodecyl chains. There have been speculations about the true compositions of the outer PC polymer surfaces under water.<sup>28,29</sup> Although the polymer surfaces may indeed contain a large fraction of dodecyl chains, long-term exposure of the polymer films to an aqueous environment may lead to a preferential expression of the PC groups onto the polymer surfaces. There is so far no direct experimental evidence to support this proposition, but the use of partially deuterated polymer will enable us to access such information in the future.

Phosphorylcholine groups are strongly hydrated,<sup>30,31</sup> and assuming that the outer surfaces of the polymer films are dominated by PC groups, the mechanism of the reduction in protein adsorption under these conditions could resemble the situation involving a layer of poly(ethylene oxide) (PEO) or poly(ethylene glycol) (PEG). Prime et al.<sup>32</sup> have systematically examined the adsorption of a number of proteins on the surfaces of PEG, PEO, or mixtures of these with alkyl chains and have attributed the effectiveness of the coated surfaces to the presence of the kinetic energy barrier arising from the steric stabilization. For the adsorption to occur, the protein molecules must overcome the hydrated water surrounding the ethoxylate groups. In the meantime, the adsorption may cause change in the configurational structure of the polymer chains. Both of these processes are considered to be unfavorable,<sup>33</sup> although from a thermodynamic point of view, dehydration may lead to the increase of system entropy and hence a decrease in the total Gibbs energy.

If, however, the contact angles for the two PC polymers remain at the intermediate values even after long-term exposure to water, the results shown in Tables 1–3 would indicate the occurrence of minimum adsorption on the surfaces with intermediate contact angles, the so-called semipolar surfaces. Note that the advancing contact angle is about  $106 \pm 4^\circ$  on OTS,  $80 \pm 3^\circ$  on PMMA, and about  $0^\circ$  on  $\text{SiO}_2$ . This is in contrast to the observation of minimum adsorption at the very hydrophilic surface by Prime et al. The only complication in our case is that, although silicon oxide represents the extreme hydrophilic surface, it is weakly negatively charged over the normal pH range.<sup>34</sup> We have, however, shown previously that the adsorption at the hydrophilic silicon oxide–water interface is dominated by the lateral steric and electrostatic repulsion, and the surface charge has no obvious correlation with any trend of adsorption under different solution pH conditions for proteins such as lysozyme and BSA.<sup>3,4</sup> The apparent discrepancy between our results and those of Prime et al. may arise from the different approaches utilized to determine protein surface excesses. In our study, all the measurements were made *in situ* at the solid–solution interface.

In comparison, Prime et al. characterized the relative extent of protein adsorption by measuring the thicknesses of the residue protein layers at the air–solid interface using ellipsometry. Prior to their ellipsometric measurements, the film surfaces were immersed in protein solution for 2 h. Once lifted out of the solution, the films were rinsed with water and were then dried in nitrogen stream. At the hydrophilic surfaces, the adsorbed proteins retain their native or globular structures. The number of contacts between protein and the substrate and between protein and its neighboring molecules is low. We have found that for this type of adsorption rinsing can partially remove those loosely adsorbed protein molecules, resulting in the underestimation of the adsorbed amount.

One of the most interesting observations in this work is the formation of the thick but diffuse protein layers at the PC 100B–solution interface. For all the three proteins studied, the thicknesses of the adsorbed layers vary from 60 to 100 Å, and the volume fractions of the proteins are always under 0.1. It is difficult to explain this phenomenon at this stage, partly because the exact composition of the outer PC polymer surface is unknown and partly because little information is available regarding the general interaction between a charge protein and a zwitterionic polymeric substrate. Although neutron reflection measurements offer no direct indication about the physical and biological nature of the adsorbed proteins under these conditions, the loose distributions of the protein layers suggest few contacts between protein molecules and the surface. It is hence likely that the adsorbed lysozyme and BSA may still retain their globular entities although fibrinogen must have lost its native structure because it is much greater in size and less stable.

## Conclusions

Coating a thin film of copolymer incorporated with phosphorylcholine and alkyl chain groups can reduce the adsorption of proteins. On the model surfaces such as silicon oxide and PMMA, the adsorbed amount shows a dramatic increase with the size and instability of protein molecules, e.g., change from lysozyme to fibrinogen. In contrast, the opposite trend was found on the two PC polymer surfaces, showing that the PC polymers are more effective at reducing the adsorption of less stable proteins.

Despite the large difference in the structure of the two PC polymer films, their effectiveness in the reduction of protein adsorption is comparable, indicating that the chemical composition of the polymers on the outer surfaces is close and the difference in the volume fraction of water does not affect the adsorption. The presence of silyl cross-linkers and the hydroxy groups does not appear to change the efficiency of the PC polymers in reducing protein adsorption.

Since the silyl cross-linking network has led to the formation of a uniform polymer film, the surface has presented a good model for examining the distributions of residue proteins adsorbed. The determination of the fragment distributions across the polymer film using partially deuterated polymers in our future work will allow a direct correlation to be made between protein adsorption and the exact surface composition of the polymer. This information will help to understand the nature of surface biocompatibility.

**Acknowledgment.** We thank the Engineering and Physical Sciences Research Council (EPSRC) for support. E.M. thanks Biocompatibles Ltd. for a studentship.

## References and Notes

- (1) Haynes, C. A.; Norde, W. *Colloid Surf. B: Biointerfaces* **1994**, *2*, 517.
- (2) Horbett, T. A.; Brash, J. L. *Protein at Interfaces II*; ACS Symp. Ser. 602; American Chemical Society: Washington, DC, 1995.
- (3) Su, T. J.; Lu, J. R.; Cui, Z. F.; Thomas, R. K.; Penfold, J. *J. Phys. Chem. B* **1998**, *102*, 8100.
- (4) Su, T. J.; Lu, J. R.; Thomas, R. K.; Cui, Z. F.; Penfold, J. *Langmuir* **1998**, *14*, 438.
- (5) Lu, J. R.; Su, T. J.; Thomas, R. K. *J. Colloid Interface Sci.* **1999**, *213*, 426.
- (6) Prime, K.; Whitesides, G. M. *Science* **1991**, *252*, 1164.
- (7) Ferguson, G. S.; Chaudhury, M. K.; Biebuyck, H. A.; Whitesides, G. M. *Macromolecules* **1993**, *26*, 5870.
- (8) Haynes, C. A.; Norde, W. *J. Colloid Interface Sci.* **1995**, *169*, 313.
- (9) Andrade, J. D. *Surface and Interfacial Aspects of Biomedical Polymers*; Plenum: New York, 1988; Vol. 2.
- (10) Hayward, J.; Chapman, D. *Biomaterials* **1984**, *5*, 135.
- (11) Lee, E. M.; Thomas, R. K.; Penfold, J.; Ward, R. *J. Phys. Chem.* **1989**, *93*, 381.
- (12) Murphy, E. F.; Lu, J. R.; Brewer, J.; Russell, J.; Penfold, J. *Langmuir* **1999**, *15*, 1313.
- (13) Murphy, E. F.; Keddie, J.; Lu, J. R.; Brewer, J.; Russell, J. *Biomaterials* **1999**, *20*, 1501.
- (14) Rowan, L. PCT/GB98/00070, WO 98/30615 (16 July 98). Also: Lewis, A. L.; Allan, C. G.; Cumming Z. L.; Goreish, H.; Kirkwood, L.; Rowan, L.; Tolhurst, L. *Biomaterials*, in press.
- (15) Azzam, R. M. A.; Bashara, N. M. *Ellipsometry and Polarised Light*; North-Holland: Amsterdam, 1977.
- (16) Lu, J. R.; Lee, E. M.; Thomas, R. K. *Acta Crystallogr.* **1996**, *A52*, 11.
- (17) Lu, J. R.; Thomas, R. K. *J. Chem. Soc., Faraday Trans.* **1998**, *94*, 995.
- (18) Su, T. J.; Lu, J. R.; Thomas, R. K.; Cui, Z. F.; Penfold, J. *J. Colloid Interface Sci.* **1998**, *203*, 419.
- (19) Morrissey, B. W.; Stromberg, R. R. *J. Colloid Interface Sci.* **1974**, *46*, 152.
- (20) Lindon, J. N.; McManama, G.; Kushner, L.; Merrill, E. W.; Salzman, E. W. *Blood* **1986**, *68*, 355.
- (21) Murphy, E. M. Ph.D. Thesis, University of Surrey, 1999.
- (22) Lu, J. R.; Su, T. J.; Thirtle, P. N.; Thomas, R. K.; Rennie, A. R. *J. Colloid Interface Sci.* **1998**, *206*, 212.
- (23) Whalgren, M.; Arnebrant, T.; Lundstrom, L. *J. Colloid Interface Sci.* **1995**, *175*, 506.
- (24) McGuire, J.; Wahlgren, M.; Arnebrant, T. *J. Colloid Interface Sci.* **1995**, *170*, 182.
- (25) Claesson, P. M.; Blomberg, E.; Froberg, J. C.; Nylander, T.; Arnebrant, T. *Adv. Colloid Interface Sci.* **1995**, *57*, 161.
- (26) Haynes, C. A.; Sliwinsky, E.; Norde, W. *J. Colloid Interface Sci.* **1994**, *164*, 394.
- (27) Fair, B. D.; Jamieson, A. M. *J. Colloid Interface Sci.* **1980**, *77*, 525.
- (28) Ruiz, L.; Hilborn, J. G.; Leonard, D.; Mathieu, H. J. *Biomaterials* **1998**, *19*, 987.
- (29) Yianni, Y. P. In *Structural and Dynamic Properties of Lipids and Membranes*; Quinn, P. J., Cherry, R. J., Eds.; Portland Press: London, 1992.
- (30) Granfeldt, M. K.; Miklavic, S. J. *J. Phys. Chem.* **1991**, *95*, 6351.
- (31) Sheng, Q.; Schulten, K.; Pidgeon, C. *J. Phys. Chem.* **1995**, *99*, 11018.
- (32) Prime, K.; Whitesides, G. M. *J. Am. Chem. Soc.* **1993**, *115*, 10714.
- (33) Sato, T.; Ruth, R. *Stabilisation of Colloidal Dispersions by Polymer Adsorption*; Marcel Dekker: New York, 1980.
- (34) Iler, R. K. *The Chemistry of Silica*; Wiley: New York, 1979.

MA991642D